J Biol Inorg Chem (2005) 10: 732–738
DOI 10.1007/s00775-005-0019-z

ORIGINAL ARTICLE

Changyuan Lu · Willem H. Koppenol

Inhibition of the Fenton reaction by nitrogen monoxide

Received: 22 March 2005 / Accepted: 8 August 2005 / Published online: 6 October 2005

Abstract The toxicity of iron is believed to originate from the Fenton reaction which produces the hydroxyl radical and/or oxoiron(2+). The effect of nitrogen monoxide on the kinetics of the reaction of iron(II) bound to citrate, ethylenediamine-*N*,*N*′-diacetate (edda), ethylenediamine-*N*,*N*,*N*′,*N*′-tetraacetate (edta), (*N*-hydroxyethyl)amine-*N*,*N*′,*N*′-triacetate (hedta), and nitrilotriacetate (nta) with hydrogen peroxide was studied by stopped-flow spectrophotometry. Nitrogen monoxide inhibits the Fenton reaction to a large extent. For instance, hydrogen peroxide oxidizes iron(II) citrate with a rate constant of 5.8×10^3 M^{-1} s^{-1}, but in the presence of nitrogen monoxide, the rate constant is 2.9×10^2 M^{-1} s^{-1}. Similar to hydrogen peroxide, the reaction of *tert*-butyl hydroperoxide with iron(II) complexes is also efficiently inhibited by nitrogen monoxide. Generally, nitrogen monoxide binds rapidly to a coordination site of iron(II) occupied by water. The rate of oxidation is influenced by the rate of dissociation of the nitrogen monoxide from iron(II).

Keywords Fenton reaction · Inhibition · Kinetics · Nitrogen monoxide · Stopped-flow spectrophotometry

Abbreviations ATP: Adenosine triphosphate · edda: Ethylendiamine-*N*,*N*′-diacetate · edta: Ethylenediamine-*N*,*N*,*N*′,*N*′-tetraacetate · hedta: (*N*-hydroxyethyl)amine-*N*,*N*′,*N*′-triacetate · nta: Nitrilotriacetate

Electronic Supplementary Material Supplementary material is available for this article at http://dx.doi.org/10.1007/s00775-005-0019-z

C. Lu · W. H. Koppenol (✉)
Institute of Inorganic Chemistry, Department of Chemistry and Applied Biosciences, Swiss Federal Institute of Technology, ETH Hönggerberg, Wolfgang–Pauli–Strasse 10, 8093 Zurich, Switzerland
E-mail: koppenol@inorg.chem.ethz.ch
Tel.: +41-1-6322875
Fax: +41-1-6321090

Introduction

Iron is an essential mineral but also associated with toxic effects if present in excess. The toxicity of iron may stem from the Fenton reaction [1], Reaction 1, which produces the hydroxyl radical or an oxoiron(2+) compound [2]. Either species is a powerful oxidant and damages biomolecules, which may ultimately result in cell death [3].

$$Fe^{II}L + H_2O_2 \rightarrow \begin{array}{l} LFeO^{2+} + H_2O, \text{ or} \\ Fe^{III}L + {}^{\bullet}OH + OH^- \end{array} \quad (1)$$

The toxicity of iron may also originate from its reactions with lipid hydroperoxides (ROOH, RH = lipid) [3, 4]. The alkoxy radicals produced initiate lipid peroxidation.

$$ROOH + Fe^{II}L \rightarrow Fe^{III}L + RO^{\bullet} + OH^- \quad (2)$$

$$RO^{\bullet} + RH \rightarrow ROH + R^{\bullet} \quad (3)$$

$$R^{\bullet} + O_2 \rightarrow ROO^{\bullet} \quad (4)$$

$$ROO^{\bullet} + RH \rightarrow ROOH + R^{\bullet} \quad (5)$$

Nitrogen monoxide has been reported to protect cells from oxidative damage caused by hydrogen peroxide and alkyl peroxides [5–9]. However, no mechanistic evidence has been reported. That nitrogen monoxide protects, is interesting, as the presence of nitrogen monoxide could also lead to peroxynitrite, a peracid that is a powerful oxidant [10].

We studied by stopped–flow spectrophotometry, the reaction of hydrogen peroxide and *tert*-butyl hydroperoxide, used as model of a lipid hydroperoxide, with iron(II) complexes in the presence of nitrogen monoxide. We used iron(II) complexed with citrate, ethylendiamine-*N*,*N*′-diacetate (edda), ethylenediamine-*N*,*N*,*N*′,*N*′-tetraacetate (edta), (*N*-hydroxyethyl)amine-*N*,*N*′,*N*′-triacetate (hedta), and nitrilotriacetate (nta). The spectroscopic and kinetic data suggest that a nitrosylferrate(II) com-

plex is rapidly formed. As reduction of a peroxide only proceeds when it is liganded to the iron [11], the rate of oxidation of iron(II) ought to be affected by the rate of dissociation of nitrogen monoxide.

Materials and methods

General

Atp (95–99%), citrate (99%), edta (99%), hedta (99%), and nta (99%) were received from Sigma-Aldrich. Edda (99%) was from Acros. Iron(II) sulfate heptahydrate (>99.5%) and iron(III) nitrate nonahydrate (>99%) were purchased from Fluka. Hydrogen peroxide (30%) and *tert*-butyl hydroperoxide (70%) were obtained from Merck. All other chemicals were of analytical grade. All chemicals were used as received. Water was purified with a Millipore Milli-Q unit fed with deionized water.

Nitrogen monoxide (99.5%), obtained from Linde AG, was passed through a 4 M potassium hydroxide solution, a column of potassium hydroxide pellets, and dry ice before use to remove higher nitrogen oxides such as nitrogen dioxide and dinitrogen trioxide. A nitrogen monoxide-saturated aqueous solution was prepared by bubbling nitrogen monoxide very gently for 90 min through water that had been previously deoxygenated by argon bubbling for 80 min. The required nitrogen monoxide concentration was obtained by diluting the solution with argon or dinitrogen-saturated solutions. The final nitrogen monoxide concentrations were measured with an ANTEK nitrogen monoxide analyzer (Houston, USA), with a chemiluminescence detector.

Preparation of solutions of iron complexes

Because all iron(II) complexes are extremely dioxygen-sensitive, the solutions were prepared by adding iron(II) sulfate heptahydrate to an argon-saturated solution of the ligand with phosphate as buffer. Iron(III) complexes were prepared by mixing stock solutions of iron(III) nitrate nonahydrate and different ligands.

UV/Vis spectrophotometry

Spectra were determined between 200 and 1000 nm with a double-beam SPECORD 200 (Analytik Jena) spectrophotometer at room temperature. Quartz cells (1.000 cm) were sealed with rubber septa and flushed with argon prior to filling with dioxygen-sensitive solutions.

Determination of the molar extinction coefficients of nitrosylferrate(II) complexes

Solutions with nitrogen monoxide in excess were mixed with solutions that contained different amounts of iron(II) (five or six samples), and then the absorption of the solutions was determined by UV/Vis spectrometry. The extinction coefficients were determined from the plot of the absorbance at the characteristic wavelength vs the concentrations of the nitrosylferrate(II) complex.

Stopped-flow spectrophotometry

Kinetic experiments were carried out at ambient pressure and 25.0 ± 0.1° C with Applied Photophysics stopped-flow spectrophotometer (SX17-MV and SX18-MV). pH was measured at the outlet. The mixing time was less than 2 ms. Six or seven kinetic traces were averaged to extract a pseudo-first-order rate constant from a single exponential fit. Gas-tight syringes were used to transfer solutions.

Kinetic simulations

The oxidation of iron(II) complexes by peroxides in the absence and presence of nitrogen monoxide was simulated with the help of chemical kinetics simulator (CKS) program from IBM.

Results

Effect of nitrogen monoxide on the rate of oxidation of iron(II) complexes by hydrogen peroxide

Experiments were performed with high concentrations of hydrogen peroxide that are at least five times higher than that of the iron(II) complex. It is not feasible to carry out experiments with the latter in excess, given the maximal concentration of nitrogen monoxide that can be achieved, 1.9 mM at 25°C [12], which is then halved by mixing. As shown in Fig. 1, the oxidation of iron(II) nta proceeds much slower in the presence of nitrogen monoxide. All kinetic traces exhibited first-order behavior, and the observed first–order rate constant, k_{obs}, increased linearly with the hydrogen peroxide concentration (Fig. 2). It made no difference whether nitrogen monoxide was added to the iron(II) complex or to the hydrogen peroxide solution. Rate constants are listed in Table 1 [13–15], and demonstrate that nitrogen monoxide can inhibit the Fenton reaction to a large extent.

A nitrosyl complex was observed immediately after mixing a solution of an iron(II) complex with a hydrogen peroxide–nitrogen monoxide solution. The decay of this nitrosyl complex observed at ca. 440 nm is synchronous with the formation of the corresponding iron(III) complex (Fig. 1). These results demonstrate that nitrosylferrate(II) complex is the precursor of the iron(III) complex. At low nitrogen monoxide concentrations $\left([NO^{\bullet}]/[Fe^{II}nta] < 1\right)$, a biphasic formation of

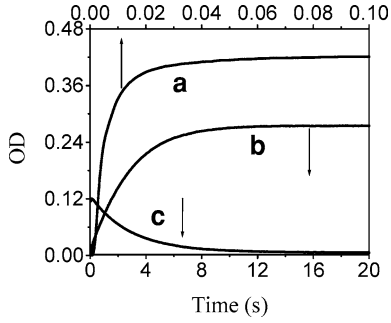

Fig. 1 Kinetics of the reaction of 0.2 mM iron(II) nta with 3.9 mM hydrogen peroxide in 6 mM phosphate buffer (pH 7.4) observed at: **a** at 300 nm in the absence of nitrogen monoxide, **b** and **c** at 300 and 440 nm, respectively, in the presence of 0.48 mM nitrogen monoxide

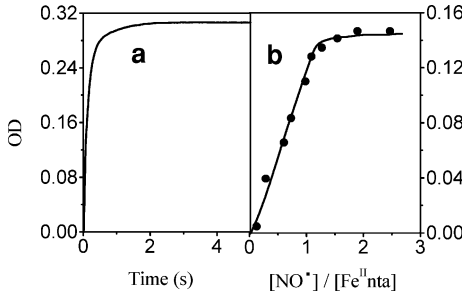

Fig. 3 **a** Kinetic trace observed at 300 nm from the reaction of 0.19 mM iron(II) nta with 4.0 mM hydrogen peroxide in the presence of 0.14 mM nitrogen monoxide and 6 mM phosphate (pH 7.4). **b** Optical density (*OD*) values observed at 440 nm obtained from the reaction of 0.19 mM iron(II) nta with 4.0 mM hydrogen peroxide (pH 7.4) in the presence of different nitrogen monoxide concentration

iron(III) nta is observed (Fig. 3a): the faster part (ms) originates from the reaction of iron(II) nta (not bound to nitrogen monoxide) with hydrogen peroxide; the slower part (seconds) is attributed to the reaction of aqua(nta)nitrosylferrate(II). Furthermore, the concentration of the species observed near 440 nm is directly related to the nitrogen monoxide concentration (Fig. 3b).

Nitrosylferrate(II) complex

Nitrosylferrate(II) complexes were prepared by mixing iron(II) complexes and nitrogen monoxide solutions. Characteristic wavelengths and extintion coefficients are listed in Table 2 and shown in Supplementary Material, Fig. S1

Nitrogen monoxide binding to iron(II) complex involves substitution of labile water molecules [16, 17]. In iron(II) deferoxamine, all the coordination sites of iron are occupied. As expected, no nitrosyl complex was observed [18].

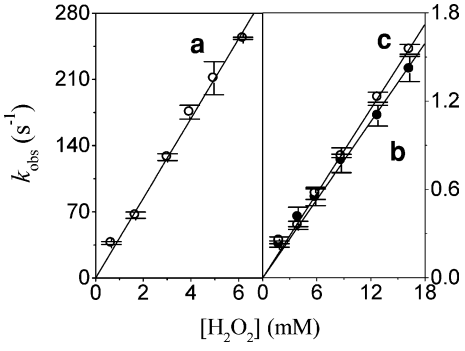

Fig. 2 Plot of the pseudo-first-order formation rates of iron(III) nta observed at 300 nm as a function of hydrogen peroxide concentration at pH 7.4 and 0.2 mM Fe(II)nta in **a**, the absence and **b**, the presence of 0.48 mM nitrogen monoxide; In **c** the decay rates observed at 440 nm in the presence of 0.48 mM nitrogen monoxide are shown

$$(H_2O)_m Fe^{II}L + nNO^{\bullet} \rightleftharpoons (NO)_n Fe^{II}L(H_2O)_{m-n} + nH_2O \quad (6)$$

To obtain information about the stoichiometry of iron(II) complexes with nitrogen monoxide, we added varying amounts of nitrogen monoxide to the solution of iron(II) complexes, followed by UV-Vis spectroscopy. The concentrations of nitrosylferrate(II) complex were plotted versus the concentration ratio $[NO^{\bullet}]/[Fe^{II}L]_{initial}$. As shown in Fig. 4, the absorbance of nitrosylferrate(II) complex increases linearly with the nitrogen monoxide concentration, until all the initial iron(II) has reacted. From the break in the curve, the stoichiometry was obtained: all iron(II) complexes shown here formed complexes with one nitrogen monoxide, except iron(II) atp, which bound to nitrogen monoxides, in agreement with previous results [19–21].

When aqua(nta)nitrosylferrate(II) was synthesized and used to study the reaction with hydrogen peroxide, the same spectral changes and kinetics were observed as in the reaction of iron(II) nta with a mixture of hydrogen peroxide and nitrogen monoxide (Table 1).

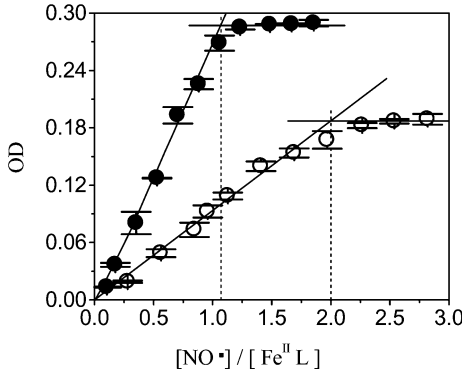

Fig. 4 Stoichiometry of the reaction of nitrogen monoxide with iron(II) nta (pH 7.4) observed at 440 nm (*filled circle*), and with iron(II) atp (pH 7.4) observed at 443 nm (*open circle*)

Table 1 Reaction rate constants of iron(II) complexes with hydrogen peroxide in the absence (argon-saturated) or presence of 0.48 mM nitrogen monoxide and 6 mM phosphate buffer (pH 7.4) at 25 °C

	Ar (k $M^{-1}s^{-1}$)		$NO^{\bullet}$ (k $M^{-1}s^{-1}$)	
	$k_{Iron(III)}\uparrow_{Literature}$	$k_{Iron(III)}\uparrow_{This\ work}$	$k_{Iron(III)}\uparrow$	$k_{Nitrosyliron(II)}\downarrow$
Fe^{II} edta	1.4×10^4 [2]	$(1.2\pm0.1)\times10^4$	6.5 ± 0.2	8.1 ± 0.3
Fe^{II} hedta	4.2×10^4 [2]	$(8.2\pm0.2)\times10^4$	13 ± 1	11 ± 1
Fe^{II} citrate	4.9×10^3 [14]	$(5.8\pm0.5)\times10^3$	$(2.9\pm0.2)\times10^2$	$(2.5\pm0.2)\times10^2$
Fe^{II} edda	7.8×10^4 [13]	$(7.9\pm0.1)\times10^4$	28 ± 1	23 ± 1
Fe^{II} nta	3×10^4 [13]	$(4.1\pm0.1)\times10^4$	83 ± 3^a	92 ± 2^a
			80 ± 1^b	90 ± 1^b
			81 ± 2^c	93 ± 3^c

↑ Formation of iron(III) complex. ↓ Decay of nitrosyl complex.
[a] Fe^{II} nta was premixed with $NO^{\bullet}$, then reacted with H_2O_2
[b] H_2O_2 was premixed with $NO^{\bullet}$, then mixed with Fe^{II}nta.
[c] NO–Fe^{II}nta(H_2O) reacted directly with H_2O_2

Table 2 Literature data on rate constants (k_a,$k_{a\text{-}1}$), stability constants (K_{NO} = $k_a/k_{a\text{-}1}$), and UV data for $(NO)_nFe^{II}L$. Spectral data at pH 7.4 were obtained in this work

Complex	Fe^{II}:L[a]	$Fe^{II}L:NO^{\bullet}$[b]	Buffer pH	k_a(M^{-1} s^{-1})	$k_{a\text{-}1}$ (s^{-1})	K_{NO} (M^{-1})	UV data ($\lambda(\epsilon)$: nm (M^{-1} cm^{-1}))
Fe^{II} edta	1:1.25	1:1 [19]	5.0	2.4×10^8 [19]	91 [19]	2.1×10^6 [19]	342(1080), 435(820), 633(130) [16]
	1:1.3	1:1	7.4	1.7×10^8 [19]			341(1079), 436(839), 633(134)[d]
Fe^{II} hedta	1:1.25	1:1 [19]	5.0	6.1×10^7 [19]	4.2 [19]	1.1×10^7 [19]	344(1080), 434(815), 634(130) [16]
	1:1.3	1:1	7.4	3.1×10^8 [19]			347(965), 437(793), 633(126)[d]
Fe^{II} citrate	1:2.3	1:1 [20]	5.0			2.1×10^4 [16]	338(1120), 443(710), 575(175) [16]
	1:5.3	1:1	7.4	4.4×10^5 [25][c]			337(1058), 442(652), 579(154)[d]
Fe^{II} edda	1:1.25		5.7			3.3×10^5 [16]	341(975), 437(920), 620(135) [16]
	1:1.3	1:1	7.4				343(921), 441(892), 622(138)[d]
Fe^{II} nta	1:2.5	1:1 [19]	5.0	2.1×10^7 [19]	9.3 [19]	1.8×10^6 [19]	342(1230), 439(870), 600(150) [16]
	1:1.4	1:1 [21]	7.4	1.6×10^7 [19]			344(1140), 441(752), 600(154)[d]
Fe^{II} atp	1:5.3	1:2	7.4				340(1010), 453(592), 597(190)[d]

[a] Fe^{II} :L indicates the ratio between iron(II) and ligand used to prepare the nitrosylferrate(II) complex.
[b] $Fe^{II}L:NO^{\cdot}$, indicates the ratio between Fe^{II} L and $NO^{\bullet}$ determined by spectroscopic methods.
[c] The rate constant was determined with a ratio of Fe^{II} to citrate of 1:1.
[d] Values obtained in this work

Effect of nitrogen monoxide on the reaction of iron(II) complex with tert-butyl hydroperoxide

Iron(II) citrate and iron(II) nta were used to investigate the inhibitory effect of nitrogen monoxide on the reduction of *tert*-butyl hydroperoxide, which was present at least in tenfold excess. The oxidation of the iron(II) complexes was first-order in *tert*-butyl hydroperoxide (Fig. 5). Similar to the results obtained with hydrogen peroxide, the reaction was much slower in the presence of nitrogen monoxide (Table 3) [4]. Within an experimental error, the rates of nitrosyl complex disappearance were in agreement with the rates of iron(III) complexes formation.

Kinetic simulations

The kinetic traces of the reactions of iron(II) complexes with hydrogen peroxide or *tert*-butyl hydroperoxide in the presence of nitrogen monoxide were simulated with the program CKS program (Scheme 1). We found that the reaction of iron(II) bound to edta, hedta, and citrate can be simulated very well with mechanism *a*, and

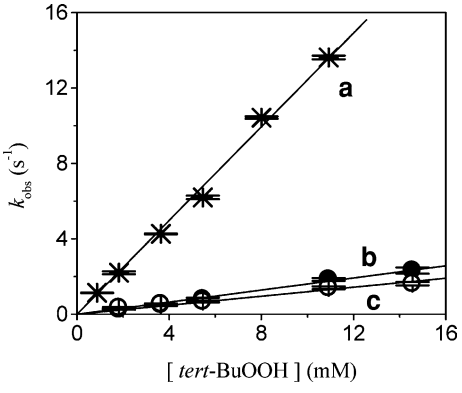

Fig. 5 Plot of the pseudo-first-order formation rates of iron(III) citrate observed at 300 nm as a function of [*tert*-BuOOH] in 6 mM phosphate buffer (pH 7.4) in **a**, the absence and **b**, the presence of 0.48 mM nitrogen monoxide, respectively; **c**, the decay rates observed at 440 nm in the case of 0.48 mM nitrogen monoxide

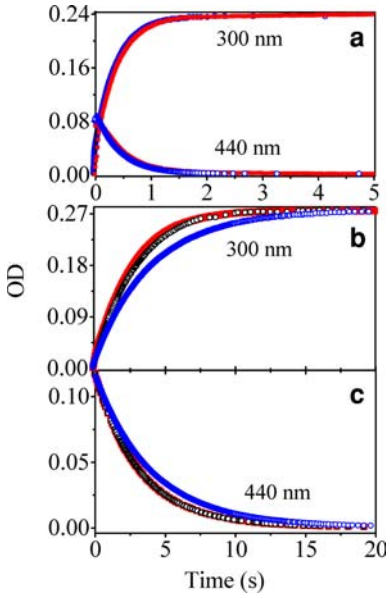

Fig. 6 Kinetic trace observed from the reaction of 0.18 mM iron(II) citrate with 5.9 mM hydrogen peroxide (**a**), and 0.2 mM iron(II) nta with 3.9 mM hydrogen peroxide (**b**) in the presence of 0.48 mM nitrogen monoxide and 6 mM phosphate (pH 7.4). Kinetic simulation with mechanism a (open circle) and mechanism b (open circle) (please see text scheme 1)

the reaction of iron(II) nta follows mechanism *b*; however, the oxidation of iron(II) edda could not be simulated by either mechanism *a* or *b* (Fig. 6 and Supplementary Material, Figs. S2, S3, S4, S5, S6).

Discussion

In principle, there are three possibilities for nitrogen monoxide to interfere with the reaction of iron(II) with peroxides: (1) Nitrogen monoxide reacts directly with the peroxide, (2) it scavenges the hydroxyl radical or oxoiron(2+), or (3) it reacts with the iron(II) complex to form a nitrosylferrate(II) complex, which reacts either directly, but slowly, with the peroxide, or after dissociation of nitrogen monoxide and binding of the peroxide to iron(II).

Nitrogen monoxide does not react with hydrogen peroxide [9, 22], and this possibility will not be discussed further. Only kinetic studies can distinguish path (2) from (3). Because the rate constants of the reactions of oxoiron(2+) and hydroxyl radical with nitrogen monoxide are ca. $1.0\times10^{7}\ M^{-1}\ s^{-1}$ [23] and $1.0\times10^{10}\ M^{-1}\ s^{-1}$ [24], respectively, much larger than that of the reaction of iron(II) complex with hydrogen peroxide [13–15], we would have found the same rate constants for the Fenton reaction in the presence and absence of nitrogen monoxide if path (2) were operative. As this is not the case, we conclude that path (3) is correct. Given the high rate constants for the reaction of nitrogen monoxide with iron(II) complexes, k_a is ca. $10^{5}\sim10^{8}\ M^{-1}\ s^{-1}$ [16, 19, 25], nitrogen monoxide reacts with iron(II) complexes before hydrogen peroxide does under our experimental conditions. One could add that if pathway (2) is correct, nitrogen monoxide would still not protect in vivo. given the low physiological concentration of nitrogen monoxide (micromolar concentration at best) and the high reactivity of the hydroxyl radical [26], scavenging of the latter by the former is kinetically unlikely.

The rapid formation of a nitrosyl complex after mixing and the observation that the decay of this nitrosyl complex is synchronous with the formation of the iron(III) complex clearly demonstrate that the nitrosylferrate(II) complex is the major iron(II) species in solution. As indicated above, the same results were obtained when a nitrosylferrate(II) complex reacted with hydro-

Mechanism a:

$$Fe^{II}L + NO^{\bullet} \underset{k_{a-1}}{\overset{k_a}{\rightleftharpoons}} NO\text{-}Fe^{II}L$$

$$Fe^{II}L + H_2O_2\,(ROOH) \xrightarrow{k_b} H_2O\,(ROH) + LFeO^{2+} \text{ or } {}^{\bullet}OH\,(RO^{\bullet}) + Fe^{III}L + OH^{-}$$

$$LFeO^{2+} / {}^{\bullet}OH\,(RO^{\bullet}) + NO^{\bullet} + OH^{-} \xrightarrow{k_c} Fe^{III}L + H_2O + NO_2^{-}\,(RONO)$$

Mechanism b:

$$Fe^{II}L + NO^{\bullet} \underset{k_{a-1}}{\overset{k_a}{\rightleftharpoons}} NO\text{-}Fe^{II}L$$

$$NO\text{-}Fe^{II}L + H_2O_2\,(ROOH) \xrightarrow{k_d} Fe^{III}L + H_2O + NO_2^{-}\,(RONO)$$

Scheme 1

Table 3 Rate constants of iron(II) complexes with *tert*-butyl hydroperoxide in the absence (argon-saturated) or presence of 0.48 mM nitrogen monoxide and 6 mM phosphate buffer (pH 7.4) at 25 °C

	Ar (k M^{-1} s^{-1})		$NO^{\bullet}$ (k M^{-1} s^{-1})	
	$k_{Iron(III)}\uparrow_{Literature}$	$k_{Iron(III)}\uparrow_{This\ work}$	$k_{Iron(III)}\uparrow$	$k_{Nitrosyliron(II)}\downarrow$
Fe^{II} citrate	1.8×10^3 [4]	$(1.4\pm0.1)\times10^3$	$(1.5\pm0.1)\times10^2$	$(1.2\pm0.1)\times10^2$
Fe^{II} nta		$(1.1\pm0.2)\times10^4$	17 ± 1	23 ± 1

↑ Formation of iron(III) complex. ↓ Decay of nitrosyl complex

gen peroxide, or when an iron(II) complex reacted with a mixture of hydrogen peroxide and nitrogen monoxide. Nitrosylferrate(II) complexes are also involved in the alkylhydroperoxide reductions.

Because the Fenton reaction proceeds when the peroxide is bound to iron(II) [2, 11], the replacement of water bound to the iron(II) by more slowly-exchanging nitrogen monoxide should attenuate the Fenton reaction. The reactions of (edta)nitrosylferrate(II), (hedta)nitrosylferrate(II), and (citrate)nitrosylferrate(II) with hydrogen peroxide and *tert*-butyl hydroperoxide follow this prediction, which is summarized in mechanism *a* in Scheme 1. Supporting evidence for this mechanism comes from a plot of the observed rate constant as a function of the nitrogen monoxide concentration. While mechanism *b* does not require saturation, mechanism *a* does. Given the attainable nitrogen monoxide concentration, only the beginning of saturation could be observed (Supplementary Material, Fig. S7). Because aqua(nta)nitrosylferrate(II) possesses a readily dissociable water molecule and nitrogen monoxide is rather tightly bound, [19, 21], it is likely that the water, and not the nitrogen monoxide, dissociates to allow binding of hydrogen peroxide or *tert*-butyl hydroperoxide (mechanism *b*). Aqua(edda)nitrosylferrate(II) also possesses a readily dissociable ligand, water, and the nitrogen monoxide is more loosely bound (Table 2), The reaction is not satisfactorily simulated by either mechanism, and we speculate that both mechanisms may operate in parallel.

The discovery of physiological roles for nitrogen monoxide changes the position of iron in the field of dioxygen toxicity. At the site of excess nitrogen monoxide and superoxide formation, such as an activated macrophage, the production of peroxynitrite ($k(NO^{\bullet} + O_2^{\bullet-}) = 1.6 \times 10^{10}\,M^{-1}\,s^{-1}$) [27] would divert superoxide from dismutation, and therefore from forming hydrogen peroxide. Furthermore, excess nitrogen monoxide would bind to iron(II) and slow the Fenton reaction. These considerations would suggest that the Fenton reaction under these conditions is less likely than the formation of peroxynitrite. The caveat must be made that the precise nature of redox-active iron is not known, and therefore rate constants and equilibrium constants are unknown.

In summary, nitrogen monoxide can attenuate the reaction of an iron(II) complex with hydrogen peroxide and alkyl hydroperoxide, in that, often, nitrogen monoxide has to dissociate from the iron(II) complex. There does not appear to be a relation between the activity and the electrode potentials. Given the results of the simulations, the number and nature of the donor atoms appears to be important. Of all the complexes examined, only the iron citrate and the iron-atp complex may be biologically relevant. The iron(II) form of the former has the lowest affinity for nitrogen monoxide, as listed in Table 2. This implies that if iron-citrate is identical to redox-active iron, then the inhibition by nitrogen monoxide will be much less pronounced. When the nature of redox-active iron has been finally elucidated, the results presented here may be helpful in understanding how it reacts with peroxides.

Supplementary Material

Spectra of nitrosylferrate complexes, kinetic simulations of the reactions of iron(II) complexes of edta, hedta, and edda with hydrogen peroxide in the presence of nitrogen monoxide, and the reactions of iron(II) bound to citrate and nta with *tert*-butyl hydroperoxide. Furthermore, the kinetics of reactions of iron(II)citrate with hydrogen peroxide at various nitrogen monoxide concentrations.

Acknowledgements This work was supported by the ETH, the Swiss National Science Foundation, and the Bundesamt für Bildung und Wissenschaft (BBW 01.0397, European Union 5th Framework project: Nutrient Iron Toxicity, QLK1-CT-2002-00444). We are indebted to Mr. P. Latal and Dr. R. Kissner for technical support.

References

1. Fenton HJH (1894) J Chem Soc, Trans 65:899–910
2. Koppenol WH (2000) Iron Chelators. In: Badman DG, Bergeron RJ, Brittenham GM (eds) New development strategies. The Saratoga Group, Ponte Vedra Beach, pp 3–10
3. Winterbourn CC (1995) Toxicol Lett 82–83:969–974
4. Rush JD, Koppenol WH (1990) FEBS Lett 275:114–116
5. Kanner J, Harel S, Granit R (1991) Arch Biochem Biophys 289:130–136
6. Kagan VE, Kozlov AV, Tyurina YY, Shedova AA, Yalowich JC (2001) Antioxid Redox Signal 3:189–202
7. Mohanakumar KP, Hanbauer I, Chiueh CC (1998) J Chem Neuroanatom 14:195–205
8. Wink DA, Hanbauer I, Krishna MC, DeGraff W, Gamson J, Mitchell JB (1993) Proc Natl Acad Sci USA 90:9813–9817

9. Farias-Eisner R, Chaudhuri G, Aeberhard E, Fukuto JM (1996) J Biol Chem 271:6144–6151
10. Beckman JS, Koppenol WH (1996) Am J Physiol Cell Physiol 271:C1424-C1437
11. Graf E, Mahoney JR, Bryant RG, Eaton JW (1984) J Biol Chem 259:3620–3624
12. Wilhelm E, Battino R, Wilcock RJ (1977) Chem Rev 77:219–262
13. Rush JD, Koppenol WH (1988) J Am Chem Soc 110:4957–4963
14. Rush JD, Maskos Z, Koppenol WH (1990) FEBS Lett 261:121–123
15. Yamazaki I, Piette LH (1990) J Biol Chem 265:13589–13594
16. Schneppensieper T, Finkler S, Czap A, van Eldik R, Heus M, Nieuwenhuizen P, Wreesmann C, Abma W (2001) Eur J Inorg Chem 491–501
17. Wolak M, van Eldik R (2002) Coord Chem Rev 230:263–282
18. Kazmierski WM, Wolberg G, Wilson JG, Smith SR, Williams DS, Thorp HH, Molina L (1996) Proc Natl Acad Sci USA 93:9138–9141
19. Schneppensieper T, Wanat A, Stochel G, Goldstein S, Meyerstein D, van Eldik R (2001) Eur J Inorg Chem 2317–2325
20. Griffiths EA, Chang SG (1986) Ind Eng Chem Fundam 25:356–359
21. Shepherd RE, Sweetland MA, Junker DE (1997) J Inorg Biochem 65:1–14
22. Koppenol WH (1996) Methods Enzymol 268:7–12
23. Herold S, Rehmann FJK (2001) J Biol Inorg Chem 6:543–555
24. Seddon WA, Fletcher JW, Sopchyshyn FC (1973) Can J Chem 51:1123–1130
25. Littlejohn D, Chang SG (1982) J Phys Chem 86:537–540
26. Buxton GV, Greenstock CL, Helman WP, Ross AB (1988) J Phys Chem Ref Data 17:513–886
27. Nauser T, Koppenol WH (2002) J Phys Chem A 106:4084–4086